PERGAMON

International Journal of Heat and Mass Transfer 41 (1998) 3575–3588

International Journal of HEAT and MASS TRANSFER

The evolution of laminar jets of Herschel–Bulkley fluids

Ijaz H. Jafri†, George C. Vradis*

Department of Mechanical, Aerospace, and Manufacturing Engineering, Polytechnic University, Six Metrotech Center, Brooklyn, NY 11201, U.S.A.

Received 12 March 1997; in final form 27 December 1997

Abstract

The steady, incompressible, non-isothermal submerged jet of a non-Newtonian Herschel–Bulkley (yield/power-law) fluid is studied using a numerical solution of the governing boundary layer equations. Emphasis is placed in determining the effects that the governing non-dimensional flow parameters, i.e. the yield number, power-law index, and Prandtl number have on the evolution of the hydrodynamic and thermal characteristics of such jets. Both yield-pseudoplastic and yield-dilatant fluids are studied for planar and axisymmetric geometries. These results show that for fluids exhibiting a yield stress, mixing is much more rapid as compared to that of yield-stress-free fluids. Moreover, the results establish the near independence of the decay of the centerline temperature from the power-law index.

Nomenclature

b non-dimensional half-jet width, $R_{1/2}/D$
C_p specific heat at constant pressure
D jet orifice diameter
k fluid thermal conductivity
K fluid consistency index
n power-law index
Pr Prandtl number, $\mu_{ref}C_p/k$
r non-dimensional radial coordinate, R/D
$r_{1/2}$ non-dimensional radial coordinate, $R/R_{1/2}$
R radial or transverse coordinate
$R_{1/2}$ half-width of the jet
Re Reynolds number, $\rho U_o D/\mu_{ref} = \rho U_o^{2-n} D^n/K$
T non-dimensional temperature; $(T^* - T_a^*)/(T_{in}^* - T_a^*)$
T^* dimensional temperature
T_a^* dimensional temperature of ambient fluid
T_c non-dimenisonal center-line temperature
T_{in}^* dimensional temperature of fluid issuing from the orifice
u non-dimensional axial velocity, U/U_o
U velocity in axial direction
U_c non-dimensional centerline velocity
U_o bulk velocity at the orifice
v non-dimensional radial velocity, $V Re/U_o$
V velocity in radial or transverse direction
x non-dimensional axial coordinate, $X/D\,Re$
X axial coordinate
Y non-dimensional yield number, $\tau_0 D/\mu_{ref}U_o$.

Greek symbols

μ_{eff} non-dimenisonal viscosity, $Y/(\partial u/\partial r) + (\partial u/\partial r)^{n-1}$
μ_{eff}^* dimensional effective viscosity
μ_{ref} reference viscosity, $K(U_o/D)^{n-1}$
ρ fluid density
τ shear stress
τ_o yield stress.

1. Introduction

Due to their large viscosities under normal processing conditions the flow of non-Newtonian fluids, such as polymer solutions and melts, is typically laminar. Therefore, in contrast to Newtonian jets which are mostly turbulent, non-Newtonian jets are usually laminar. The motivation for studying jets of non-Newtonian fluids has been the need to analyze and understand the underlying fluid mechanics and heat transfer phenomena associated with the mixing processes involving such fluids.

* Corresponding author. Tel: 001 516 755 4350; fax: 001 516 755 4526; e-mail: gvradis@poly.edu.

† Presently R & D Projects Engineer, GT Equipment Technologies, Inc., 472 Amherst Street, Nashua, NH 02063, U.S.A.

0017–9310/98 $19.00
PII: S0017–9310(98)00050–7

Early on the theoretical investigation of laminar jet mixing was primarily focused on similarity solutions of the governing equations. The similarity solution for a Newtonian jet was presented by Schlichting [1]. The same approach was later extended to non-Newtonian power-law fluids by a variety of researchers who proved the existence of a similarity solution in such cases. Lemieux and Unny [2] employed the boundary layer equations to obtain an analytical solution for the flow of a laminar, two-dimensional, incompressible, submerged, pseudo-plastic jet. A non-linear second-order ordinary differential equation was obtained through a similarity transformation and a numerical solution was employed to this equation. As a result, the similarity solution given in [1] for a Newtonian jet was established as a special case of the more general analysis presented in [2]. Atkinson [3] presented a closed form solution for the same case by employing an analytical approach. Atkinson reported a disagreement between his results and those given in [2] when the power-law index was equal to or less than one-half ($n < 0.5$). This, according to Atkinson [3], was a consequence of the assumption made by Lemieux and Unny [2] that the volume rate of discharge was infinite for power-law indices less than or equal to one half.

Using a similarity transformation and employing a numerical solution to the resulting third order ordinary differential equation (using a Runge–Kutta–Gill fourth order forward integration routine) Rotem [4] presented results for the case of an axisymmetric free laminar jet of an incompressible pseudoplastic fluid. The results presented in [4] showed that the similarity solution to the boundary layer equations becomes invalid for values of the power-law index equal to or less than 0.5, fact attributed to the assumption made in the similarity formulation that the orifice radius is zero at the origin. Gutfinger and Shinner [5] conducted an analytical as well as an experimental study for the same problem. The results predicted by theory failed to reproduce those obtained by experiments, however the discrepancies can be attributed to the differences in the rheology of the modeled and the tested fluids. For the axisymmetric jet of a power-law fluid Serth [6] presented a numerical solution for an ordinary differential equation obtained from the boundary layer equations using a similarity transformation. Experimental results for the evolution of centerline velocity using a hot film probe were also presented. An observed sharp decline in the velocity close to the exit plane was attributed to the viscoelatsic properties of the working fluid (Separan AP 30). Mitwally [7] employed a similarity transformation followed by a numerical solution of the resulting second order differential equation for flow configurations covering the two-dimensional plane and radial free jets, the axisymmetric free jet, and the plane and radial wall jets. The last two studies [6, 7] both indicated that the jet of a pseudoplastic fluid decays faster as compared to the jet of a dilatant fluid.

Vlachopoulos and Stournaras [8] presented a numerical solution for the evolution of the steady laminar plane jet of a power-law fluid. Utilizing the concept of the 'effective viscosity', results were obtained showing an excellent agreement with the respective similarity solution in the region far downstream from the jet's development region. The differences between the results in [8] and those given by the similarity results of Lemieux and Unny [2] in the developing region are due to the inherent assumptions in similarity solutions, which fail to accurately predict the flow in the early stages of the jet's evolution. However, as the distance from the orifice increases, the numerical results asymptotically approach those of the similarity solution.

Using a Milling Yellow solution and exploiting its birefringent properties Kumar et al. [9] conducted experimental work which resulted in the development of correlation between the non-dimensional laminar length (laminar length/orifice diameter) and the jet's Reynolds number for pseudoplastic jets:

$$1 = 9.5 \times 10^{7} Re^{-2.23} \quad 650 < Re < 1100 \tag{1}$$

Rubel [10] presented a solution for a planar liquid wall jet by solving the full Navier–Stokes equations to implement the boundary conditions in the entire domain. These results reaffirmed that the boundary layer solution is highly accurate, for all engineering purposes, at high Reynolds numbers.

Jordan et al. [11] presented an experimental and theoretical study of a submerged laminar pseudoplastic jet. Separan AP30 solutions of different concentrations were used in conjunction with the non-intrusive Laser Doppler Anemometry (LDA) technique to obtain experimental results for the decay of center-line velocity. Two different rheological models namely the power-law and power-series viscosity models were employed to solve the governing continuity and momentum equations using an implicit finite differences scheme. It was concluded that the power-series viscosity model prediction was in better agreement with the experimentally obtained velocity data than the power-law viscosity model. However, these models were unable to provide good prediction for jet growth rates given the viscoelastic properties of the working fluid.

Recently attention has been focused in understanding the behavior of jets of non-Newtonian fluids exhibiting a yield stress due to the increased importance of such fluids in many industrial applications, including mixing processes and the re-suspension of settled slurries and colloidal dispersions in tanks containing waste of various processes. Such fluids are complex from a rheological point of view, generally exhibiting pseudoplastic behavior with a yield stress. Terrones and Eyler [12] conducted a numerical study in which it was assumed that the propagation of the laminar non-Newtonian jet is identical to the turbulent Newtonian jet. This assumption provided

satisfactory results for the overall flow characteristics of the cases studied. Trent and Michener [13] in a study of turbulent power-law jets assumed that turbulence characteristics within non-Newtonian fluids are similar to those in Newtonian fluids. Finally, in a recent study Shekarriz et al. [14] presented a preliminary study of experimental results obtained using Particle Image Velocimetry (PIV) for laminar and transitional jets of Carbopol solutions. Discussion of these last results will be presented later in greater detail due to their relevance to the present work.

The present study concentrates on studying the evolution of a Herschel–Bulkley fluid (yield-shear thinning as well as yield-shear thickening) submerged jet under steady, incompressible, laminar, non-isothermal flow conditions. The boundary layer approximations are employed in conjunction with the effective viscosity formulation to derive the momentum balance equation describing the problem. A block implicit algorithm is used to numerically solve the governing mass and momentum balance equations. Once the velocity field is obtained, the linear energy equation is solved separately. The code is validated by comparing present predictions with the available results for Newtonian, pseudoplastic, and dilatant fluids. The effects of the governing yield and Prandtl numbers as well as those of shear thinning and shear thickening rheology on the flow structure are studied.

2. Problem formulation

In this work the evolution of both an axisymmetric and a planar free submerged jet is studied. The ensuing fluid is at a temperature different from that of the stagnant ambient fluid. The governing boundary layer equations in non-dimensional form for the given problem are as follows:

$$\frac{\partial u}{\partial x}+\frac{1}{r^c}\left(\frac{1}{\partial r}(r^c v)\right)=0 \tag{2}$$

$$u\frac{\partial u}{\partial x}+v\frac{\partial u}{\partial y}=\frac{1}{r^c}\frac{\partial}{\partial r}\left(r^c\mu_{\text{eff}}\left(\frac{\partial u}{\partial r}\right)\right) \tag{3}$$

$$u\frac{\partial T}{\partial x}+v\frac{\partial T}{\partial y}=\frac{1}{Pr}\frac{1}{r^c}\frac{\partial}{\partial r}\left(r^c\left(\frac{\partial T}{\partial r}\right)\right) \tag{4}$$

(where $c=0$ and 1 for the planar and axisymmetric cases, respectively).

The concept of the effective viscosity has been used above in writing the non-dimensional governing equations. In the case of a yield/power-law fluid, i.e. a Herschel–Bulkley fluid, and for a boundary layer flow the relationship between the stress and rate of deformation is reduced to and given by:

$$\tau=\tau_0+K\left(\frac{\partial U}{\partial R}\right)^n \quad \text{for } \tau>\tau_0 \tag{5a}$$

$$\frac{\partial U}{\partial R}=0 \quad \text{for } \tau\leqslant\tau_0 \tag{5b}$$

Defining the effective viscosity μ^*_{eff} as:

$$\tau=\mu^*_{\text{eff}}\frac{\partial U}{\partial R} \tag{6}$$

the corresponding expression for the fluid defined in (5) becomes:

$$\mu^*_{\text{eff}}=\left(\frac{\tau_0}{\partial U/\partial R}\right)+K\left(\frac{\partial U}{\partial R}\right)^{n-1} \quad \text{for } \tau>\tau_0 \tag{7a}$$

$$\mu^*_{\text{eff}}=\infty \quad \text{for } \tau\leqslant\tau_0 \tag{7b}$$

As a result the non-dimensional effective viscosity is given by:

$$\mu_{\text{eff}}=\left(\frac{Y}{\partial u/\partial r}\right)+\left(\frac{\partial u}{\partial r}\right)^{n-1} \quad \text{for } \tau>\tau_0 \tag{8a}$$

$$\mu_{\text{eff}}=\infty \quad \text{for } \tau\leqslant\tau_0 \tag{8b}$$

where, the yield number Y represents a non-dimensional yield stress ($Y=\tau_o D/\mu_{\text{ref}}U_o$) and expresses the relative magnitude of the yield stress to the shear stresses.

A uniform ('top-hat') velocity and temperature profile is assumed at the tip of the orifice. The fluid exits into a stagnant and uniform temperature pool of the same fluid. Thus, at $x=0$ and for $r<1/2$, $u=T=1$, $v=0$; and at $x=0$, and for $r\geqslant 1/2$, $u=T=0$. Due to symmetry, the gradient of the axial component of the velocity and that of the temperature in the radial direction as well as the magnitude of the radial velocity component along the center-line are zero, i.e. at $r=0$; $\partial u/\partial r=\partial T/\partial r=v=0$. The boundary condition at $r\to\infty$ is realized by setting $u=T=0$ at a large distance from the jet center-line. Numerical experimentation indicates that this condition is sufficiently met at a radial distance of about 25 nozzle diameters for the domain length of interest in this study.

The governing equations are discretized using a fully second order accurate scheme. Centered differences are used for the diffusion and transverse convection terms while backward differencing is used for the streamwise convective term. The computational grid employed is that originally proposed by Welch et al. [15]. The system of discretized equations obtained is solved along each grid line in the transverse direction using an iterative technique. The non-linearities due to the effective viscosity and convective terms are removed using values from the previous iteration level. The resulting system of linear equations is solved using the block tri-diagonal solver proposed by Isaacson and Keller [16]. Thus, the solution to the problem is obtained by marching line by line from the jet exit to downstream until either similar solutions are obtained or the velocities reach very low values. In the present numerical scheme continuity is

always satisfied to 'machine accuracy' in any stage of the solution procedure. Consequently convergence is checked for the momentum and energy equations and the iterative procedure is terminated when the residuals become less than 10^{-6}. For a detailed description of the numerical technique the reader is referred to the work of Vradis and Jang [17] and Vradis and VanNostrand [18]. To ensure a grid independent solution various grid sizes and locations of the outer jet boundary were studied. The results reported here are independent of these factors within a small tolerance.

From equation (8b) it is seen that effective viscosity becomes infinite in regions of $\tau \leqslant \tau_o$ (the fluid cannot sustain a rate of deformation in such regions). The numerical implementation of equation (8b) obviously creates difficulties. Extremely large values of the effective viscosity create convergence problems because the coefficient matrix becomes very 'stiff' due to large differences in the magnitude of its elements. To circumvent such problems, a maximum value for the effective viscosity is assumed if $\partial u/\partial r \leqslant 10^{-5}$, i.e. the viscosity is frozen at a maximum value for low shearing rates. This approach has also been successfully employed by Vlachopoulos and Stournaras [8], Ozoe and Churchill [19], O'Donovan and Tanner [20], and Vradis and Hammad [21]. The effective viscosity is under-relaxed in order to warranty convergence. The results obtained with the present code have been compared and extensively verified against the numerical solutions by Pai and Hsieh [22] for Newtonian fluids and those of Vlachopoulos and Stournaras [8] for non-Newtonian power-law fluids. Excellent agreement was found with the results of both works.

3. Results and discussion

The characteristics of Herschel–Bulkley (i.e. yield-power law) jets are presented next, both for planar and axisymmetric geometries, with the yield number varying from 0–1.5, the power-law index varying between 0.6 and 1.5, and the Prandtl number varying from 1–10. The Reynolds number effects are 'removed' by introducing it in the coordinate transformation in the axial direction and the velocity transformation in the radial direction (See Nomenclature).

For purposes of comparison, the results obtained with the present algorithm for Newtonian and non-Newtonian power-law fluids (and as stated above validated against existing solutions) are shown in Fig. 1(a). The decay of the non-dimensional center-line velocity as a function of the non-dimensional axial distance clearly depends on the power-law index with a pseudoplastic fluid jet decaying faster than a dilatant fluid jet. Comparison of the axisymmetric case with the planar one indicates that the centerline velocity decays faster in the case of an axisymmetric jet, fact which is consistent with the results presented by Rotem [4]. In both the planar and the axisymmetric jet, however, the initial development of the jet, i.e. in the range of $0 < x < 0.09$, is practically independent of the power-law index. Figure 1(b) shows the non-dimensional half-jet width as a function of the non-dimensional axial distance for planar and axisymmetric geometries. Lemieux and Unny [2] and Vlachopoulos and Stournaras [8] predicted the jet expansion boundary to be concave for values of power-law index greater than 2/3 and convex for those less than 2/3, and the results obtained in this work are consistent with those of the above researchers. Notice that as the power-law index decreases, the rate at which the jet is spreading increases, this rate being higher in the case of an axisymmetric jet.

The introduction of a yield stress has a profound effect on the evolution of the jet and in particular of the axisymmetric one. Figure 2(a) shows the decay of the center-line velocity as a function of axial distance for a yield number of $Y = 0.25$ for an axisymmetric and a planar geometry. For the planar jet the break-up of the initial potential core of the jet is taking place within a substantially shorter distance from the orifice as compared to the yield-stress-free fluid. This breakup is then followed by a rapid decay of the center-line velocity, a decay which initially (for $x \leqslant 0.1$) is independent of the power-law index. For $x > 0.1$ the jet evolves faster with lower power-law indices, the differences being less pronounced than in the case of $Y = 0$. The more rapid mixing indicated by the faster evolution of center-line velocity is accompanied by the faster growth of the jet's half-width (Fig. 2(b)). The Newtonian jet shows a near linear growth of the half-width with axial distance. Pseudoplastic jets, showing a mixing rate higher than Newtonian, exhibit a faster growth of this parameter. Concentrating now on the axisymmetric case, it is seen that the rate of growth for this jet is extremely high resulting in the complete mixing of the jet fluid into the stagnant environment within a very small distance from the orifice. Thus, the introduction of a yield stress results in an extremely fast mixing process even for very low yield numbers. The axial velocity profiles are presented in Fig. 3 for the case of planar jets with a yield number of $Y = 0.25$. These axial velocity profiles, which are far downstream from the 'initial' region, clearly indicate the presence of a plug zone around the axis of symmetry where the flow is solid-body like. On decreasing the power-law index the core region where the fluid is solid-body-like increases in size and the evolution is slower as dictated by the higher effective viscosities.

On increasing the yield number from 0.25–0.5, it is noticed that even though the development of the jet in the initial region is identical, the effect of the yield number is stringently felt in the region slightly downstream of the core region. Figure 4(a) and (b) show the decay of the center-line velocity and the growth in jet half-width for

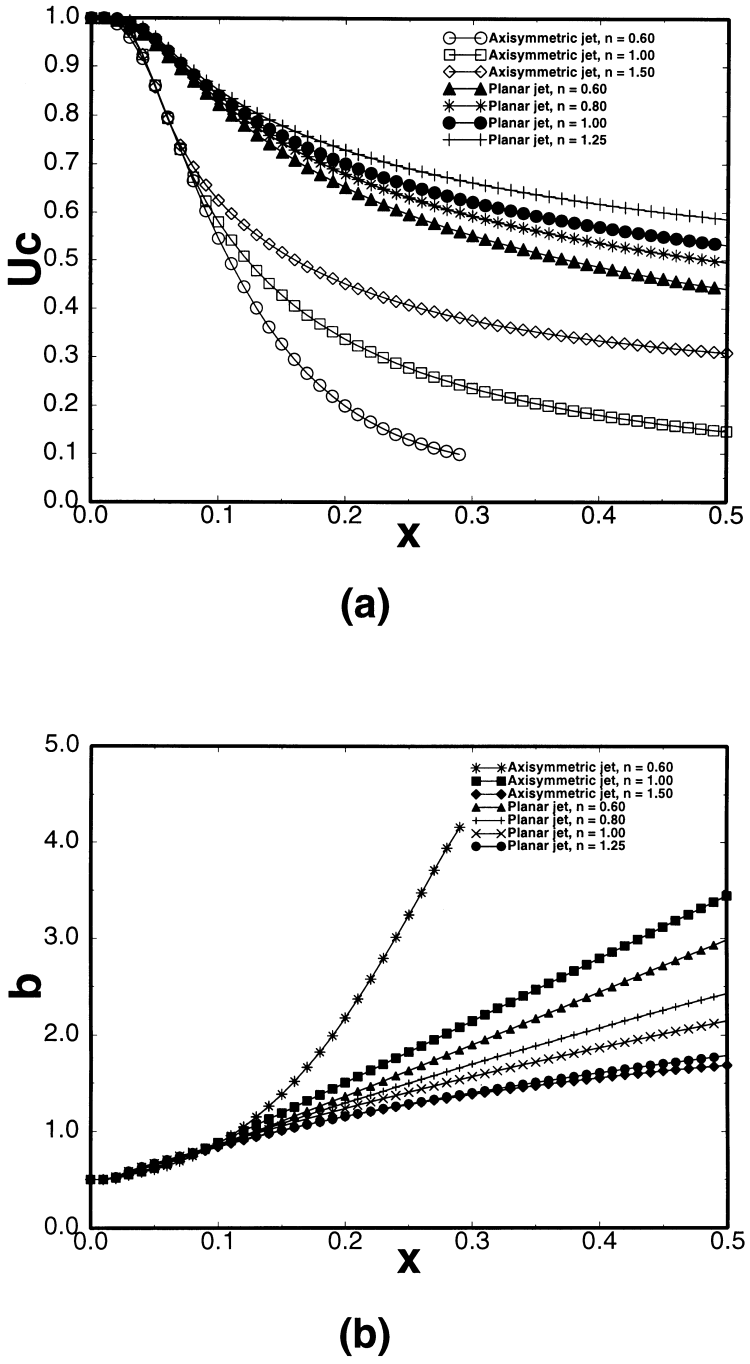

Fig. 1. Variation of: (a) non-dimensional centerline velocity; and (b) non-dimensional half-jet width with non-dimensional axial distance (yield number = 0.0).

the planar and axisymmetric jet for a yield number of $Y = 0.5$. The distributions for the center-line velocity start to collapse to a single curve and the decay is more rapid than the previous case of $Y = 0.25$. In the core and transitional regions the velocities are overlapping each other and jet decay is rapid. In the case of an axisymmetric jet, since the center-line velocity decays to near zero in the very early stages, the jet is unable to penetrate the stagnant fluid mixing with it in an extremely rapid fashion.

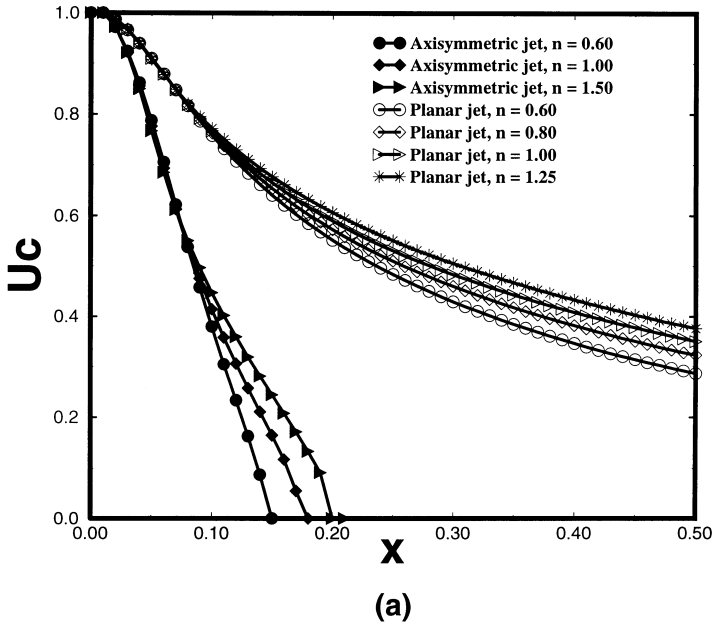

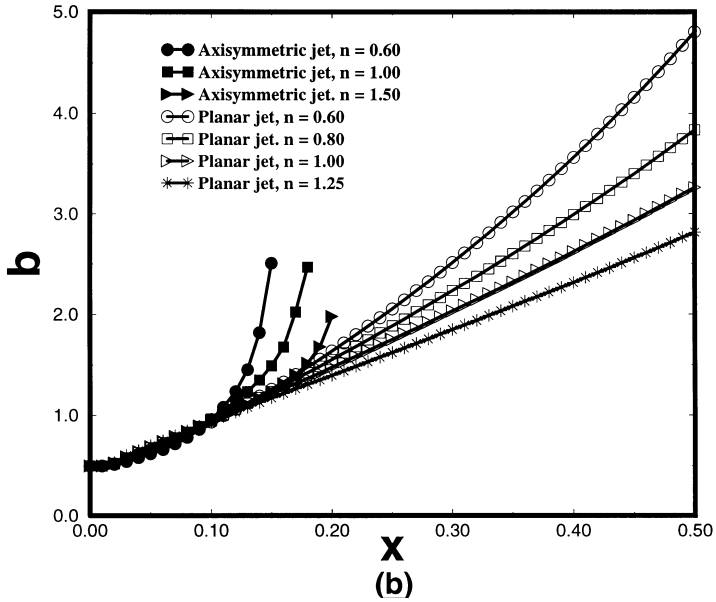

Fig. 2. Variation of: (a) non-dimensional centerline velocity; and (b) non-dimensional half-jet width with non-dimensional axial distance (yield number = 0.25).

A further increase in yield number to $Y = 1.0$ (Figs 5(a) and (b)) results in decay rates of centerline velocity which are almost independent of the power-law exponent. Thus, the evolution of the jet becomes practically independent of power-law index at higher yield numbers. This is even more so in the case of the axisymmetric jet where all curves collapse into a single one within numerical accuracy. The growth rate in this case is practically infinite. There is a large plug-zone which grows in size as the jet fluid comes almost to a stop. This plug-zone eventually grown in size and acts as a barrier that restricts the penetration of the jet.

While at a yield number of $Y = 1.0$, the center-line velocity and the half-jet width have collapsed to a single

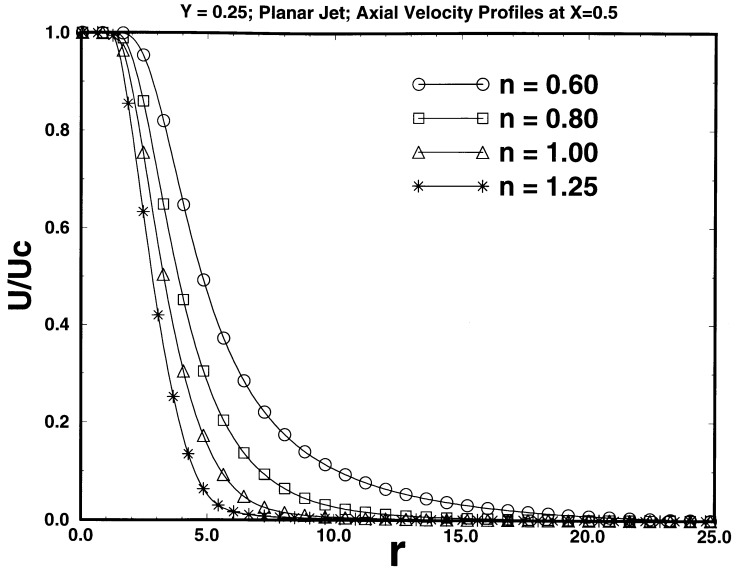

Fig. 3. Non-dimensional axial velocity vs. non-dimensional radial distance for $Y = 0.5$.

curve for an axisymmetric jet, the same is not true for a planar jet. An increase of yield number to $Y = 1.5$ for a planar jet (Figs 6(a) and (b)) shows that the centerline velocity decays to zero with all the curves overlapping and the jet width almost identical irrespective to the power-law index. The faster growth of the planar jet is associated with a rapid growth of the size of the plug-zone along the centerline. While this plug-zone is present for every yield fluid, its importance and dominance does not become evident at small yield numbers due to the fact that in those cases inertia effects control the development of the jet in the initial region. However, at higher yield numbers the inertia effects are weakened and the plug-zone along the centerline plays a very significant role in the jet's development.

The above results introduce another element in the discussion regarding the large growth rates of certain jets observed in laboratory studies. The recent study by Shekarriz et al. [14] has validated these observations in the case of Capbopol solutions, in which once the concentration of Carbopol exceeds a certain level, the growth rate of the jet becomes very high. Such behavior has been attributed to the past in the low power-law exponent exhibited by such solutions and to their viscoelastic effects. Given the fact that at the concentrations at which the rapid growth is experienced coincides with the appearance of a yield stress, the present study introduces another element in the argument, strongly indicating that such effects may be due to yield number effects. Further work is needed, however, to settle this issue.

An important element of the Newtonian and power-law fluid jets is the attainment of similarity axial velocity profiles at a relatively large distance from the jet origin. Figure 7(a) shows the axial velocity profiles for a Newtonian and two power-law fluid jets at three axial locations far downstream in the jet. As seen, in all three cases the profiles collapse on each other thus, indicating the attainment of similarity. In the case of fluids exhibiting a yield stress, no similarity is achieved as seen in Fig. 7(b) for the case of a Bingham plastic ($n = 1$). Similar results have been obtained for all cases of Herschel–Bulkley fluids ($n \neq 1$) studied in this work as well. While the profiles are close in the vicinity of the centerline and in the far field there are substantial differences in the shear layer region. Thus, it appears that no similarity profiles exist in the case of yield stress exhibiting fluids.

The temperature decay history, used here to demonstrate the evolution of a scalar field in such jets, is obtained for different cases. Figure 8(a) shows the decay of center-line temperature for a Newtonian fluid and for Prandtl numbers of 1.0, 5.0, and 10.0. As expected, for a Newtonian fluid the temperature and velocity decays are identical for a Prandtl number of $Pr = 1.0$ (both planar and axisymmetric). As with the momentum transfer, the energy (temperature) transfer is faster in the case of the axisymmetric jet. Higher Prandtl numbers are associated with a slower decay in centerline temperature. On increasing the Prandtl number, the energy (thermal) dissipation via molecular diffusion becomes less dominant, thereby, the spreading or distribution of energy is primarily through convection. A further increase in Prandtl number clearly indicates that the dissipation of thermal energy becomes extremely slow. This is clearly evident in the case of a Prandtl number of $Pr = 10$ and a Newtonian

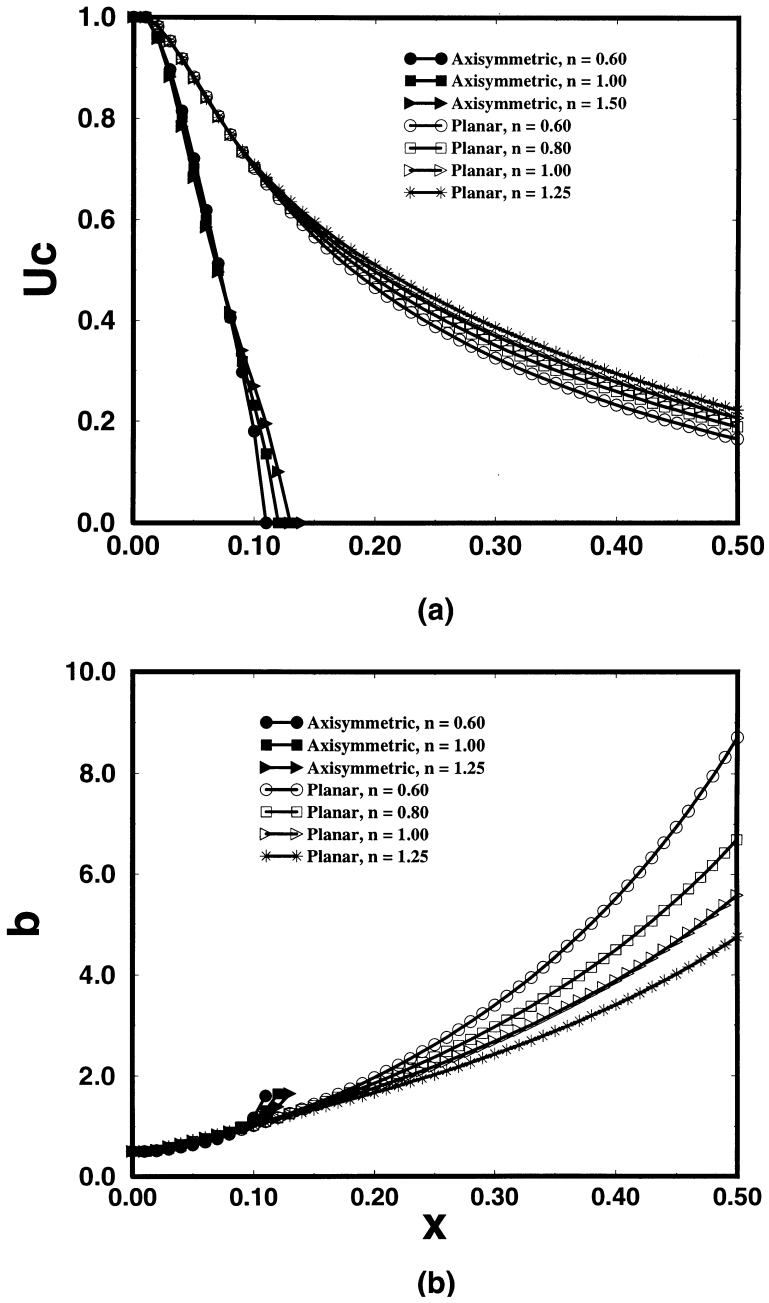

Fig. 4. Variation of: (a) non-dimensional centerline velocity; and (b) non-dimensional half-jet width with non-dimensional axial distance (yield number = 0.50).

fluid (Fig. 8(a)). To study the influence of the yield number on the temperature field (which is dependent on the velocity field), the yield numbers of 0.5 and 1.0 are selected for a planar geometry (see Fig. 8(b)). The introduction of a yield stress results in a slowdown in the evolution of the temperature field. In the plug-zone region along the centerline of the jet, the only mode of heat transfer is conduction (due to the lack of shear). This results in a purely conductive heat transfer mechanism in this region and thus, low heat transfer rates. As the Prandtl number increases, the internal heat capacity storage of the fluid is increased while the thermal conductivity

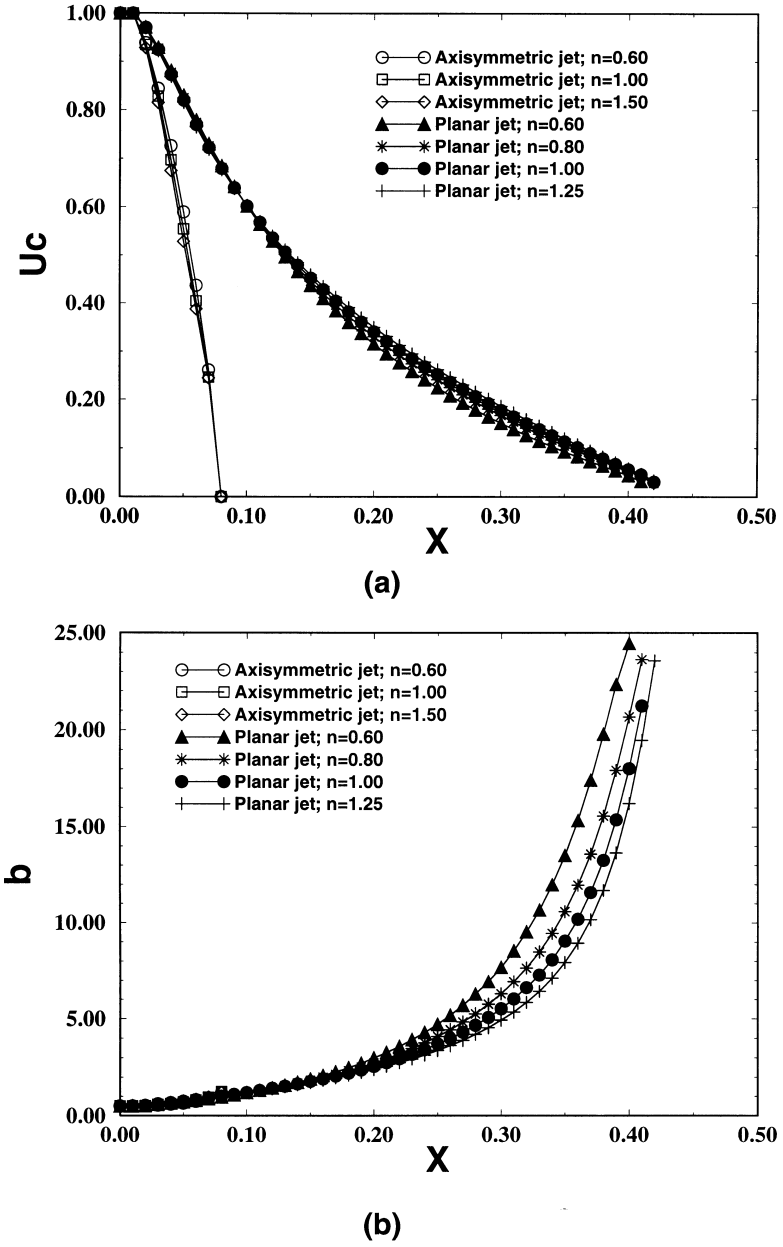

Fig. 5. Variation of: (a) non-dimensional centerline velocity; and (b) non-dimensional half-jet width with non-dimensional axial distance (yield number = 1.00).

is further reduced and hence there is very less dissipation via diffusion. As a result even lower rates of decay of the centerline temperature are experienced. For Prandtl numbers greater than ten, the rate of decay becomes very low. From these results it is obvious that the yield number effect is much weaker than that of the Prandtl number (for low Prandtl numbers). Next the effect of the power-law index on the thermal field is shown in Fig. 9. The dissipation of thermal energy is primarily a function of Prandtl number and nearly independent of yield number or power-law index. In this analysis for Prandtl numbers of 1 and 5, the power-law index is varied keeping the yield number constant at $Y = 0.5$. Thus, while the velocity development is dependent on both the power-law index

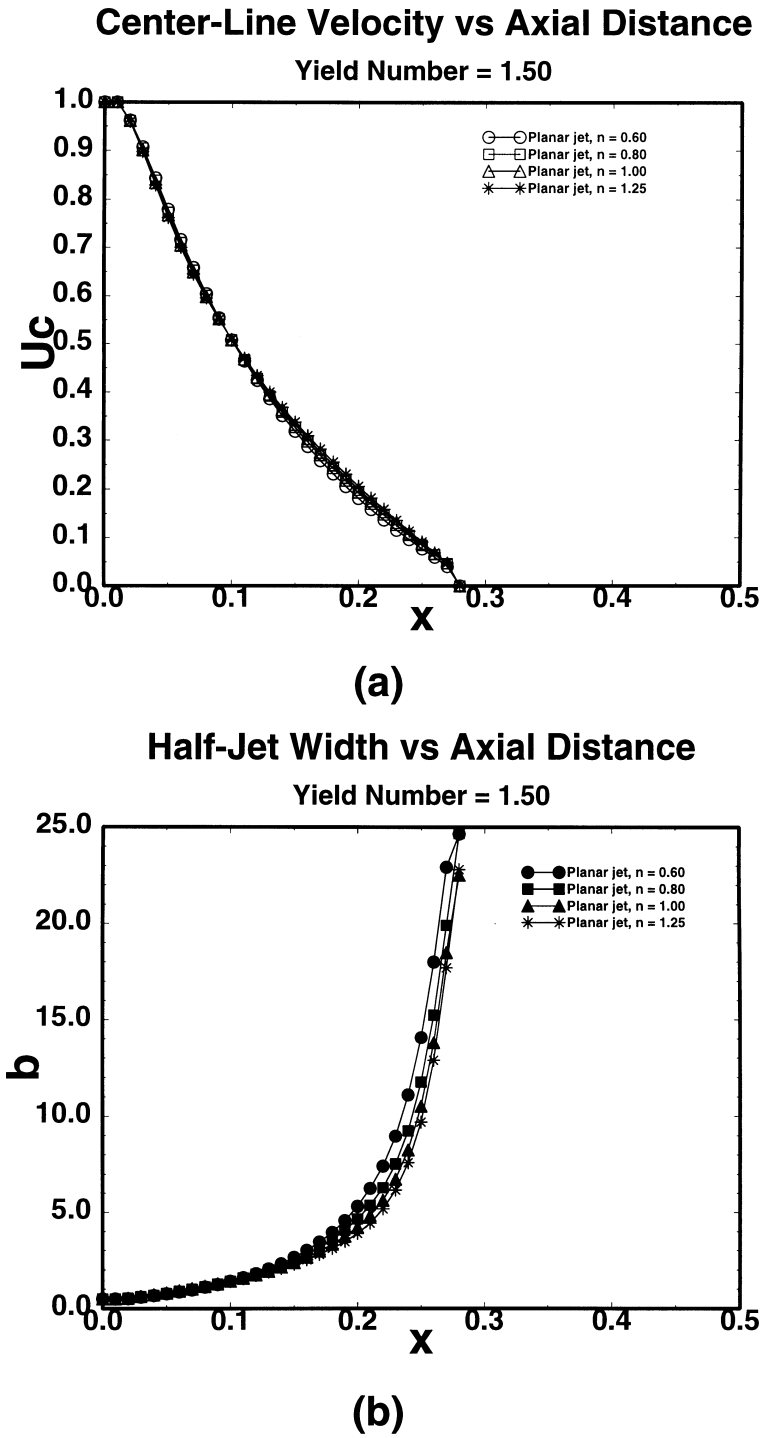

Fig. 6. Variation of: (a) non-dimensional centerline velocity; and (b) non-dimensional half-jet width with non-dimensional axial distance for a planar jet (yield number = 1.50).

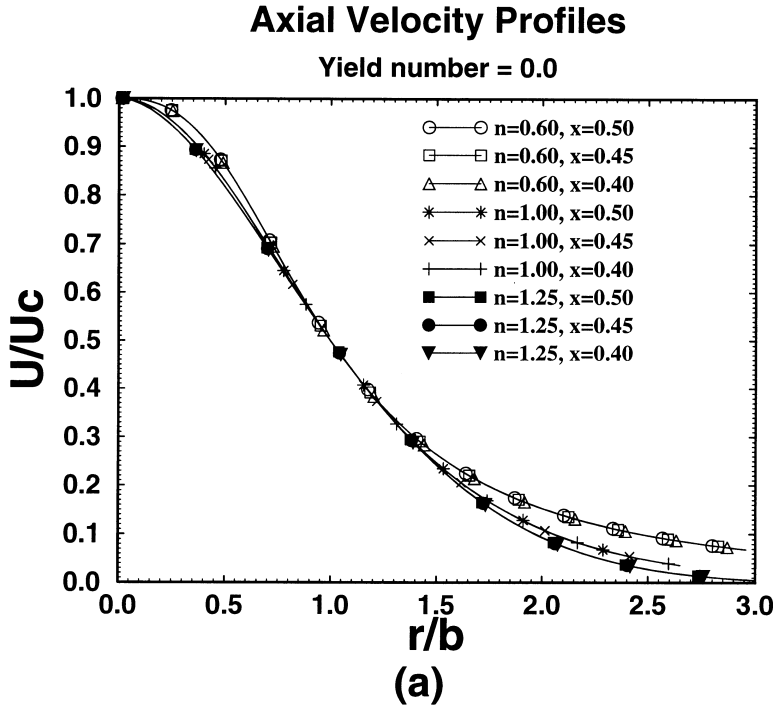

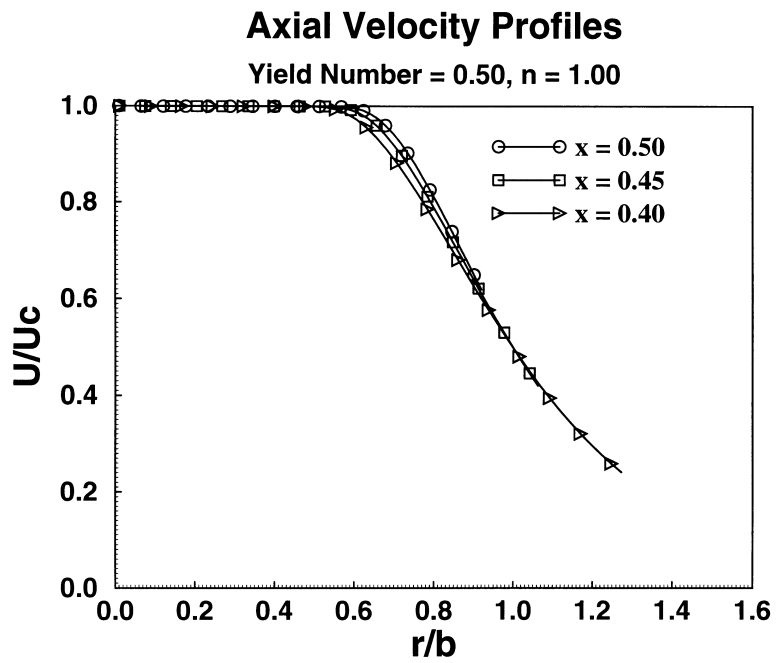

Fig. 7. Non-dimensional axial velocity profiles in the far downstream region: (a) $Y = 0$, $n = 0.6$, 1.0, and 1.25; and (b) $Y = 0.5$, $n = 1.0$.

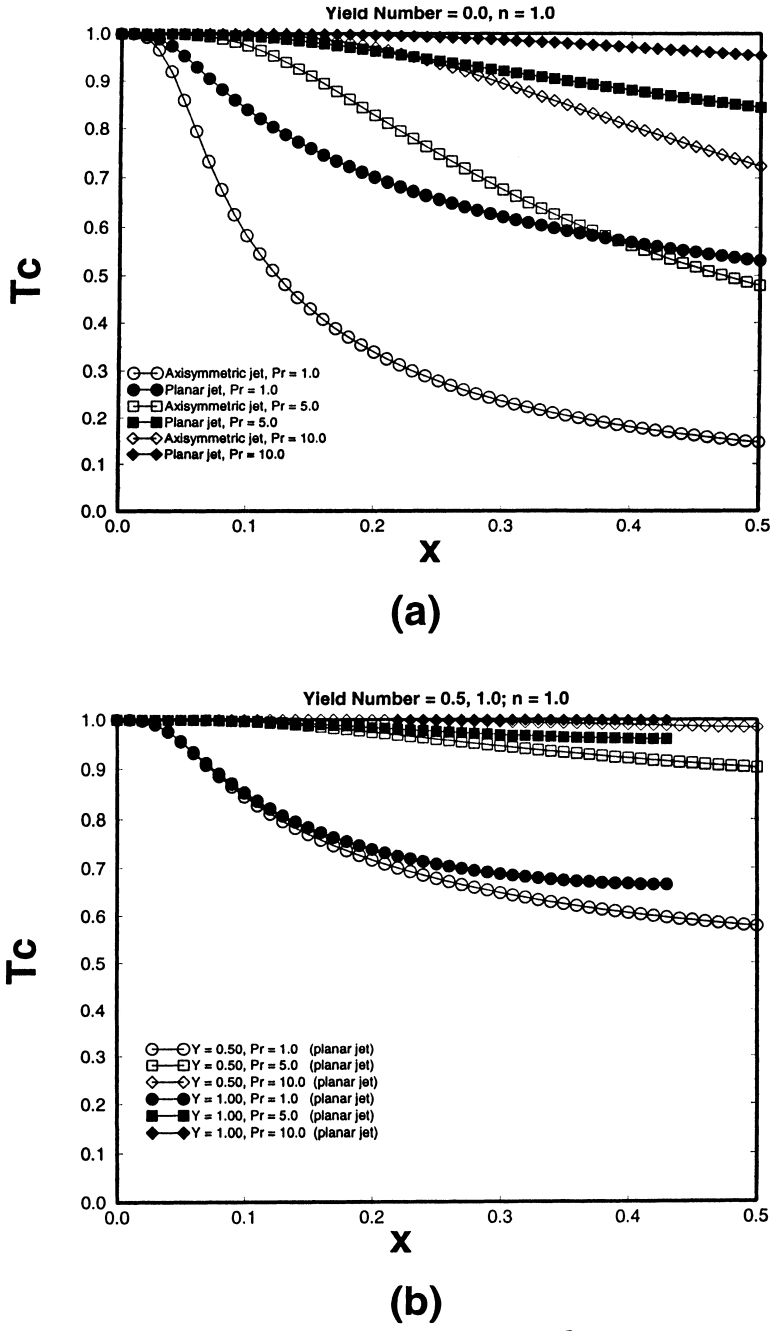

Fig. 8. Non-dimensional centerline temperature vs. non-dimensional axial distance: (a) $Y = 0.0$, $n = 1.0$; and (b) $Y = 0.5$ and 1.0; $n = 1.0$.

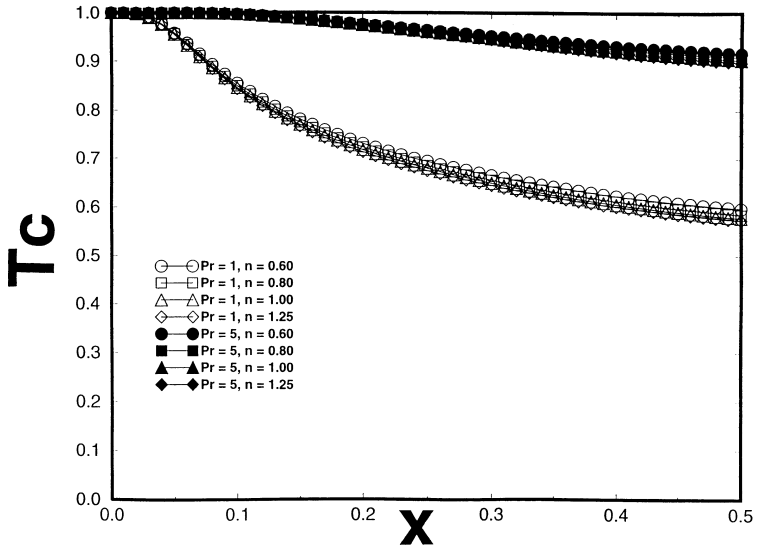

Fig. 9. Non-dimensional centerline temperature vs. non-dimensional axial distance for a planar jet of $Y = 0.50$, $Pr = 1$, and 5, and $n = 0.6$, 0.8, 1.0 and 1.25.

and the yield number, the temperature development is nearly independent of these two factors, especially at higher Prandtl numbers.

4. Conclusion

The present work focused on the analysis of the axisymmetric and planar non-isothermal jet of an incompressible, inelastic, yield-stress exhibiting fluid. Results are presented for yield-dilatant and yield-pseudoplastic fluids. The results obtained indicate that the jet expansion boundary becomes concave to the jet axis for all flows exhibiting high yield numbers. The results also show the independence of the decay of the centerline velocity from the power-law index for such fluids for relatively high yield numbers. The evolution of a jet is identical and independent of yield number in the initial stages of jet development. The plug-zone present along the center-line dominates the flow evolution away from the inlet region. It is also shown that for yield stress exhibiting fluids no similarity profiles ever develop in the far-field region of the flowfield. In addition it is shown that the decay of the jet's centerline temperature becomes independent of the power-law index and the yield number, especially for high Prandtl number fluids.

References

[1] Schlichting H. Boundary Layer Theory, 6th ed. New York : McGraw-Hill, 1968.

[2] Lemieux PF, Unny TE. The laminar two-dimensional free jet of an incompressible pseudoplastic fluid. Journal of Applied Mechanics, Trans ASME, 90 1968;35:810.

[3] Atkinson C. On the laminar two-dimensional free jet of an incompressible, pseudoplastic fluid. Journal of Applied Mechanics, Trans ASME, 94 1972;39:1162.

[4] Rotem Z. The axisymmetric free laminar jet of an incompressible pseudoplastic fluid. Applied Science Research 1964;A13 :353.

[5] Gutfinger C, Shinner R. Velocity distributions in two-dimensional laminar liquid-into-liquid jets in power-law fluids. AIChE Journal, 1964;10(5):631–9.

[6] Serth RW. The axisymmetric free laminar jet of a power-law fluid. Journal of Applied Mathematics and Physics 1972;23:131–8.

[7] Mitwally EM. Solutions of laminar jet flow problems for non-Newtonian power-law fluids. Journal of Fluids Engineering 1978;100:363–6.

[8] Vlachopoulos J, Stournaras C. Laminar two-dimensional non-Newtonian jets. AIChE Journal 1975;21(2):385–8.

[9] Kumar KR, Rankin GW, Sridhar K. Laminar length of a non-Newtonian fluid jet. Journal of Non-Newtonian Fluid Mechanics 1984;15:13–27.

[10] Rubel A. Navier–Stokes similarity solution for the planar liquid wall jet. AIAA Journal 1987 ;25(1) :179–81.

[11] Jordan C, Rankin GW, Sridhar K. A study of submerged pseudoplastic laminar jets. Journal of Non-Newtonian Fluid Mechanics 1992;41:323–37.

[12] Terrones G, Eyler LL. Computer modeling of ORNL storage tank sludge mobilization and mixing. PNL-8855/UC-510 Report. Richland, Washington : Pacific Northwest Laboratory, 1993, pp. 5.12–5.23.

[13] Trent DS, Michener T. Numerical solution of jet mixing concepts in tank 241-SY-101. PNL-8559 Report. Richland, Washington : 1993. Pacific Northwest Laboratory.

[14] Shekarriz A, Phillips JR, Weir TD. Experimental study of a pseudoplastic jet using particle image velocimetry. ASME Advances and Applications in Laser Anemometry. 1994;FED-191:191–201.
[15] Welch JE, Harlow FH, Shannon JP, Daly BJ. The MAC method. Los Alamos Scientific Lab Report. LA-3425, 1966.
[16] Isaacson E, Keller BH. Analysis of Numerical Methods. New York : Wiley, 1966.
[17] Vradis G, Jang KS. Numerical studies for the turbulent planar jet. ME Report 91-09. Polytechnic University, 1991.
[18] Vradis G, VanNostrand L. Laminar coupled flow downstream of an axisymmetric sudden expansion. AIAA Journal of Thermophysics and Heat Transfer 1992;6(2): 288–95.
[19] Ozoe H, Churchill SW. Hydrodynamic stability and natural convection in Ostwald–de-Waele and Ellis fluids—the development of a numerical solution. AIChE Journal 1972;18:1196.
[20] O'Donovan EJ, Tanner RI. Numerical study of the Bingham squeeze film problem. Journal of Non-Newtonian Fluid Mechanics 1984;15:75–83.
[21] Vradis GV, Hammad KJ. Heat transfer in flows of Bingham fluids through axisymmetric sudden expansions and contractions. Numerical Heat Transfer Part A, 1995;28:339–53.
[22] Pai SI, Hsieh T. Numerical solution of laminar jet mixing with and without free stream. Applied Science Research 1972;27:39–62.